Atmospheric Research 138 (2014) 59–72

Contents lists available at ScienceDirect

Atmospheric Research

journal homepage: www.elsevier.com/locate/atmos

Impact of urban growth-driven landuse change on microclimate and extreme precipitation — A sensitivity study

Assela Pathirana [a,*], Hailu B. Denekew [a], William Veerbeek [b], Chris Zevenbergen [a,b], Allan T. Banda [a]

[a] UNESCO-IHE Institute for Water Education, Westvest 7, Delft 2611AX, The Netherlands
[b] Department of Hydraulic Engineering, Faculty of Civil Engineering and Geosciences, Delft University of Technology, Stewinweg 1, Delft 2628CN, The Netherlands

ARTICLE INFO

Article history:
Received 9 March 2012
Received in revised form 3 October 2013
Accepted 6 October 2013

Keywords:
Urbanisation
Urban heat island
Urban growth
Landuse change
Atmospheric model
Hydrometeorology

ABSTRACT

More than half of the humanity lives in cities and many cities are growing in size at a phenomenal rate. Urbanisation-driven landuse change influences the local hydrometeorological processes, changes the urban micro-climate and sometimes affects the precipitation significantly. Understanding the feedback of urbanisation driven micro-climatic changes on the rainfall process is a timely challenge. In this study we attempt to investigate the impact of urban growth driven landuse change on the changes in the extreme rainfall in and around cities, by means of sensitivity studies. We conduct three sets of controlled numerical experiments using a mesoscale atmospheric model coupled with a land surface model to investigate the hypothesis that the increasing urbanisation causes a significant increase of extreme rainfall values. First we conduct an ensemble of purely idealised simulations where we show that there is a significant increase of high intensity rainfall with the increase of urban landuse. Then four selected extreme rainfall events of different tropical cities were simulated with first current level of urbanisation and then (ideally) expanded urban areas. Three out of the four cases show a significant increase of local extreme rainfall when the urban area is increased. Finally, we conducted a focused study on the city of Mumbai, India: A landscape dynamics model Dinamica-EGO was used to develop a future urban growth scenario based on past trends. The predicted future landuse changes, with current landuse as control, were used as an input to the atmospheric model. The model was integrated for four historical cases which showed that, had these events occurred with the future landuse, the extreme rainfall outcome would have been significantly more severe. An analysis of extreme rainfall showed that hourly 10-year and 50-year rainfall would increase in frequency to 3-year and 22-year respectively.

1. Introduction

Today, more than half of the world's population lives in cities. Due to the increasing concentration of businesses and infrastructure, the urbanisation process continues at a phenomenal rate. The urban water cycle and the local climatic environment are invariably affected by the urban growth (Foley et al., 2005). The causal relationship between urbanisation and increased stormwater flows due to the hydrological changes on the surface is well understood and quantified. It is common knowledge that the urbanisation increases runoff due to the retardation of infiltration and evapotranspiration processes, and decreases the resistance to flow. The question whether the rainfall itself is changed due to the micro-climatic changes above cities as a consequence of urban landuse change, was being asked since the 1960s. Today, there is an increasing body of evidence that the changes in the radiation and heat balance affected by changes in surface albedo and vegetation cover on the urban micro-climate

* Corresponding author. Tel.: +31(0)15 215 1854.
E-mail address: assela@pathirana.net (A. Pathirana).

0169-8095/$ – see front matter © 2013 Elsevier B.V. All rights reserved.
http://dx.doi.org/10.1016/j.atmosres.2013.10.005

can have significant impacts on the precipitation patterns over urban centres and their surroundings (Watkins and Kolokotroni, 2013). These hydro-meteorological effects are caused by a) microphysical changes resulting from urban pollution, b) increased surface roughness due to urban structures and c) heat anomalies resulting from changes in albedo and latent heat flux — 'urban heat island (UHI)' (Sagan et al., 1979). While the urban heat island effect on radiation, temperature and wind has been documented relatively early (Taha et al. (1988), Landsberg (1981) and references therein) modelling investigations on the impact on rainfall appeared late in the literature. Some of the difficulties in the latter endeavour is summarised by Lowry (1998). There have been many empirical investigations indicating the possibility of the urban growth and the resulting UHI modulating precipitation (e.g. Shepherd, 2006; Jauregui, 1996; Subbiah et al., 1990; Lin et al., 2008, 2009; Takahashi, 2003). Of particular interest is the Metropolitan Meteorological Experiment (METROMEX), a major observational study conducted in the US in the 1970s (Changnon, 1979). METROMEX findings showed that precipitation down-wind of large cities can increase 5%–25% from background values (Shepherd, 2005). Charabi and Bakhit (2011) used meteorological data measured over a period of one year over the city of Muscat, Oman, to study the urban heat island over the city. They found that the hottest locations occur at the compactly built 'old Muscat' neighbourhoods in narrow valleys. During the rare winter rainfall spells the intensity of UHI decreased. Meir et al. (2013) examined two 2011 heat events in New York City to evaluate the predictive ability of 1 km resolution US Navy's Coupled Ocean/Atmosphere Mesoscale Prediction System (COAMPS) model and 12 km resolution North American Mesoscale (NAM) implementation of WRF model using a land and coastline based observation networks. The high resolution model was able to capture the key features of the heat events, where urban rural temperature differences were as high as 4–5 °C.

Numerical modelling experiments are extremely relevant in understanding and quantifying the possible effect of UHI on rainfall, as this is probably the only way to conduct controlled studies at city and regional scales to investigate the sensitivity of various influencing parameters. Shepherd (2005) noted that there had been relatively few studies in this field. Since then there have been a number of reports on such experiments. Shem and Shepherd (2009) conducted controlled experiments on three landuse scenarios for Atlanta, USA, with different levels of urbanisation and concluded that there is a significant impact of UHI on cumulative rainfall quantities resulting in increases of 10% to 13% for increased urbanisation. Lin et al. (2008) reported results of numerical experiments comparing impacts of UHI on rainfall by comparing the atmospheric response to synthetically increasing urban area in the case of Taiwan. They concluded that the UHI interaction with summer-time sea-breeze and mountain uplifting contributes significantly to increase rainfall in the mountainous areas on the leeward side of the city. On the other hand, analysing the 7th July 2004 thunderstorm over Baltimore, USA by means of controlled modelling studies, Ntelekos et al. (2008) concluded that UHI did not contribute to the heavy rainfall during the event.

Most of the studies in the recent literature on the UHI and precipitation had a strong focus on mesoscale meteorology, and often stopped short of making impact assessment at the urban scale. It is indeed challenging to translate the predictions of the impacts of UHI driven changes in the meteorological events to forms that can be readily used by civil engineers to plan urban water infrastructure. Such an attempt would invariably result in large uncertainties and could leave many gaps in reasoning that future research has to fill in. However, the possible strong causal link of urbanisation on urban extreme rainfall can no longer be ignored, particularly in the context of rapid urban growth and numerous external pressures like global climate change. There is a growing interest on the role of land cover and landuse change on climate change (Solomon et al., 2005), partially due to the awareness raised by events like the Nerima heavy rainfall (Kawabata et al., 2007) and general indications of significant increase of extreme rainfall in rapidly urbanising locations like the Indian subcontinent that are suspected to be triggered by UHI (Kishtawal et al., 2010). However, in order to understand the impacts on the issue of urban drainage and flooding, it is important to understand the influence of UHI on short-term, extreme rainfall — the driving force on urban storm water system. The fact that most populous cities, which happen to be in the Third World, have already over-stressed that storm drainage systems further increase the relevance of it.

In this paper, we present the results of a series of numerical experiments conducted using a state of the art, 3D mesoscale atmospheric model — WRF-ARW (Skamarock et al., 2005) — in order to attempt to understand the impact of urbanisation-driven landuse change on the extreme rainfall events in and around cities. Our hypothesis is that changes in urban landuse cause significant changes in extreme rainfall in urban centres and surrounding areas. We propose that these changes will have significant implications on the planning and implementation of urban drainage projects, mitigation of urban floods and ensuring the human security in cities in general. It should be noted that we limit the scope of this sensitivity study to the possible changes in the urban heat budget, due to changes in the thermal properties (radiative, latent heat) of urban landscape. We ignore the possible changes in boundary layer roughness (due to tall buildings) and microphysical changes due to urban pollution.

First we present the results of idealised experiments that indicate the sensitivity of increase of urban land use to rainfall and the related mechanisms. For the second set of experiments, we have selected a number of extreme rainfall events from around the world that caused significant urban flooding. We conducted 'what-if' type of analyses on these events. We introduced a simplified artificial urbanisation with the scenario that the city grows to twice its original diameter and investigate what level of influence this 'urban-growth' would have on the magnitude of rainfall. Finally, for the City of Mumbai, we conduct detailed urban growth modelling, that would give many more realistic extrapolations of landuse change during the next two decades based on historical trends and various influencing spatial parameters. We used standard statistical techniques used in rainfall frequency analysis to interpret the results in the context of urban storm drainage design and urban flooding, so as to demonstrate the practical implications of the findings.

2. WRF-ARW model

WRF-ARW model numerically solves the four conservation relationships, namely mass, momentum and heat conservation of air and mass conservation including phase changes of water, by a non-hydrostatic 3D set of equations. The model uses terrain-following vertical coordinate system and square grid horizontal coordinates with vector and scalar quantities staggered on the grid. With the initial conditions provided for the entire 3D domain and lateral boundary conditions for the entire duration of the run, the model uses an explicit 2nd/3rd order Runge–Kutta scheme to explicitly

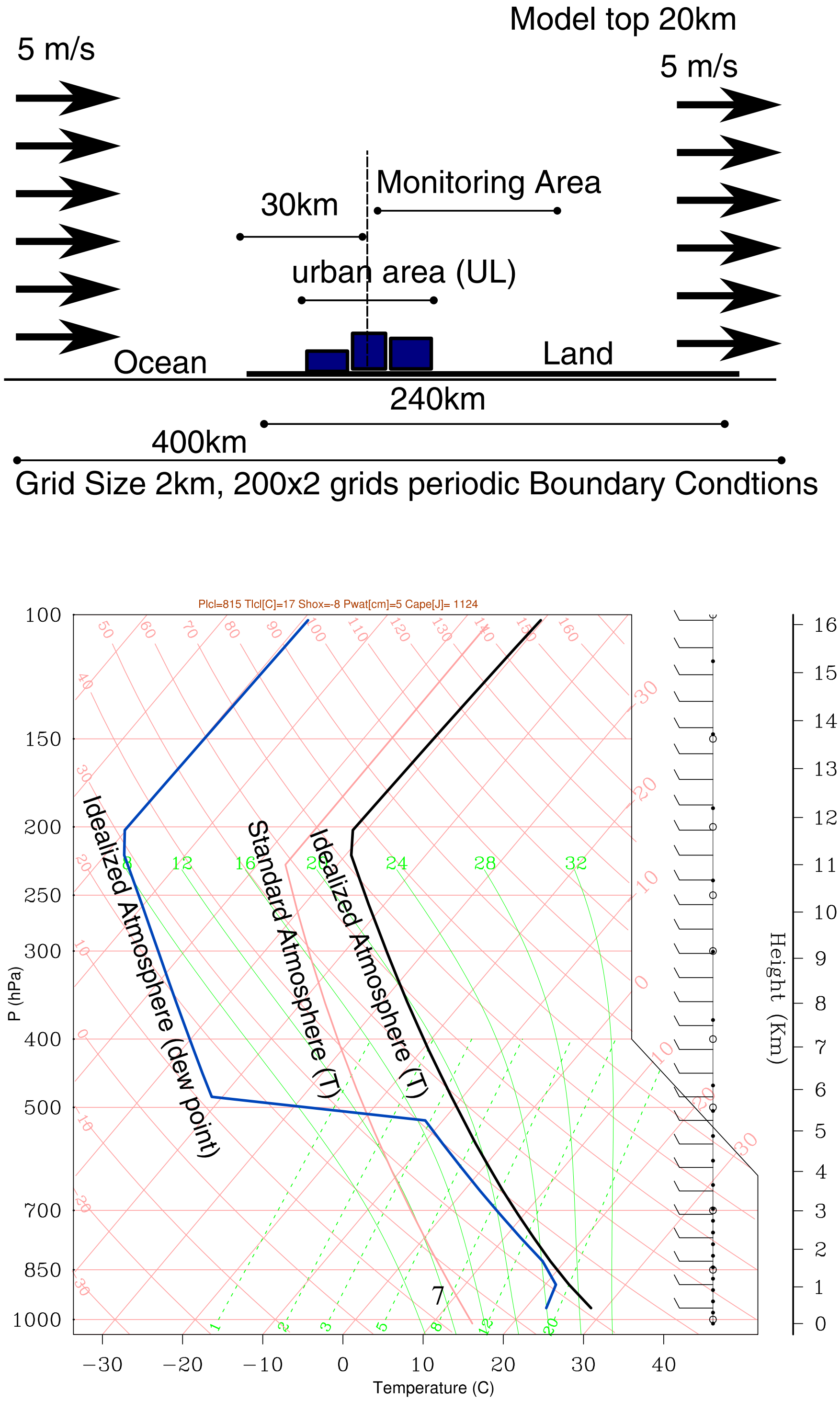

Fig. 1. The model domain for idealised experiments (top). Log-P-Skew-t plot for the atmosphere profile (bottom).

solve the system forward in time. The top boundary condition is parameterised often as a constant pressure surface and solar radiation is calculated based on the geographic location and cloud cover. The bottom boundary is provided by a surface scheme that could be a layered thermal diffusion model or a sophisticated landuse model that explicitly considers the vegetation and moisture effects of the surface. The planetary boundary layer is also modelled. The model physics include the full representation of the cloud microphysics that includes three phases of water and up to six classes of hydrometeors. The full description of the WRF-ARW model is given by Skamarock et al. (2005). The model is suitable for both operational use (e.g. weather forecasting) and research studies.

3. Idealised model

When testing a hypothesis, experimentation is arguably the most reliable approach, and the equivalent of it in large-scale environmental modelling is idealised numerical studies. Under precisely controlled conditions, repeatable numerical experiments are conducted with only a single parameter changed at a time. In the field of atmospheric science, there have been numerous applications of this technique to investigate various hypotheses (Doyle and Durran, 2001; Pathirana et al., 2005, 2007; Li, 2006). In order to test the hypothesis we stated above, we used WRF-ARW model (Skamarock et al., 2005) to simulate a 2-dimensional model domain whose essential features are illustrated in Fig. 1 (top). The domain possesses only three landuse categories: 16 — Water Bodies to represent ocean, 18 — Wooded Wetlands and 01 — Urban and Built-up Land (USGS Land Use/Land Cover System Legend). Table 1 lists important physical parameters of the three landuse types used. The model was set-up with a coupled land-surface model, Noah-LSM (Mitchell, 2000) in order to represent the vegetation and moisture effects on the surface. The lapse rate of the atmosphere in the idealised experiment was very similar in shape to that of the standard atmosphere, but the temperatures being higher values (to suit tropical conditions). The troposphere is conditionally unstable — once the surface heats up, this easily leads to convective break up. Up to about 5 km altitude the atmosphere is quite moist, in encouraging the development of rainfall. The Log P sekw-T plot is shown in Fig. 1 (bottom). Idealised domains were located at [0,0] (on the equator at 0 longitude).

Table 1
Important physical parameters associated with three landuse types.

Landuse type	Urban and built-up land	Water bodies	Wooded wetlands
USGS index (—)	1	16	18
Albedo (%)	15	8	14
Soil moisture (frac.)	0.1	1	0.35
Surface emissivity (frac.)	0.88	0.98	0.95
Roughness length (m)	0.5	0.0001	0.4
Leaf area index (—)	1	0.01	5.8
Green vegetation fraction (frac.)	0.1	0	0.6
Rooting depth (soil layer index)	1	0	2
Stomatal resistance ($s\ m^{-1}$)	200	100	100

The initial conditions were such that the entire modelling domain had a uniform 5 m/s wind field in x-direction (Fig. 1). The lateral boundary conditions were periodic in both x and y-directions. In effect this set-up recycles the wind field exiting at the end of the domain to the beginning of the domain. Since the 'ocean' stretch provided is inadequate to keep replenishing the water vapour, there is a limit to the total quantity of rainfall that the system will produce however long the simulation time is.

The model was integrated for a 12 h period with different sizes of urban area (UL from 0 (control) to 40 km, in steps of 4 km). In order to obtain a more statistically representative result, the simulations at each UL were repeated ten times with slightly different initial conditions (random perturbations of velocity, temperature and moisture). The ensemble results are shown in Fig. 2 for the 'monitoring area' (60 km stretch from the centre of the urban patch) shown in Fig. 1. The high intensity rainfall amount shows a statistically significant relationship with the amount of urbanisation. The same analysis for the rainfall of the entire modelling domain (as opposed to the 60 km monitoring area) did not show a statistically significant trend of rainfall with urbanisation (not shown). Furthermore, the rainfall in the region windward of the urban patch showed a statistically significant reduction of high intensity rainfall.

All the experiments started at 05:50 local time (05:50 GMT). The initial surface temperature was set uniformly: 287 K for ocean and 290 K for land. The model setup considers solar heating of surface (using MM5 short-wave radiation scheme). The 'sunrise' occurs soon after the model starts. In around 3 h the surface starts to heat up as the sun rises. The heat build-up is faster on the urban patch resulting in convective activity aloft (Fig. 3(left)). The resulting convective break-up aids in developing rainfall initially in the lee-side of the urban patch within an hour (Fig. 3 (right)).

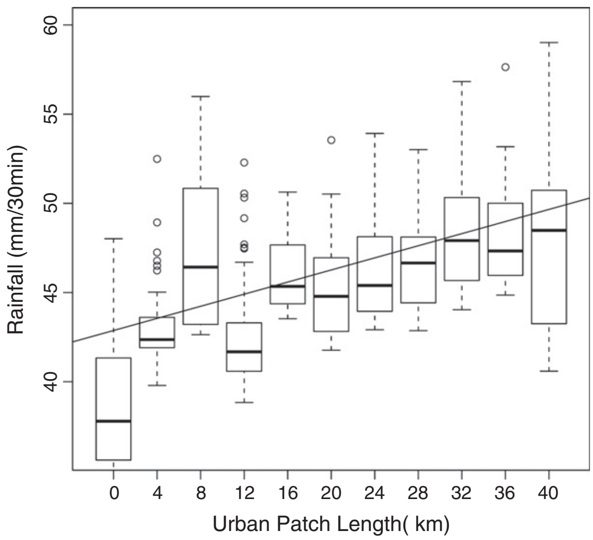

Fig. 2. The largest 25% of grid-level rainfall observed over the 60 km monitoring area. All 30 min rainfall values of each ensemble set (i.e. all simulations for a specific length of urban patch) were pooled and sorted in the order of descending intensities. Then the first 25% were used to produce the corresponding box plot.

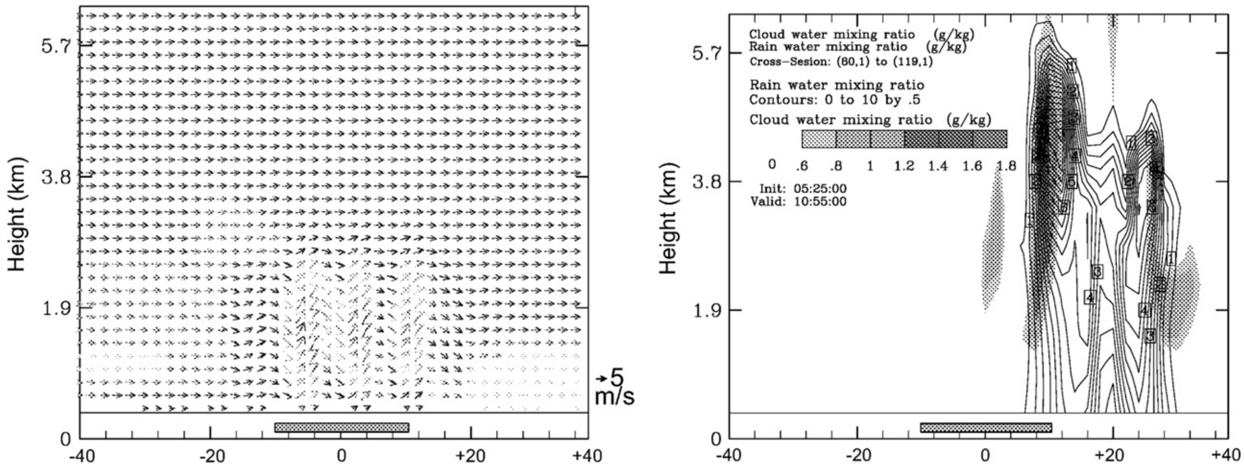

Fig. 3. Cross sections of a simulation with 20 km urban patch. Left: wind vectors at 09:55 h (with vertical exaggeration of 50) shows the initiation of convective activity aloft the urban patch (grey bar). Right: cloud formation and rainfall at 10:55 h. The precipitation starts at the lee-side of the urban-patch.

4. Semi-idealised case studies

For the second phase of the study, we selected four Asian cities of varied sizes, that have had faced urban floods due to local heavy precipitation during the last decade (Table 2). The objective of the second phase was to ascertain, in the case of historical rainstorms, whether the extreme rainfall outcome would be significantly different, if these events would happen in a situation where a large urban growth has taken place. At this stage we did not attempt to realistically model the urban growth of each city, but considered a situation where the urban landuse has filled an area twice the current city size ('Future scenario'). Fig. 4 shows the implemented change for the case of the city of Colombo. In this experiment the urban expansion introduced was not realistic by any means. How this change was implemented in the model is explained in the following section. The control experiments (the 'Present scenario') were conducted using the current landuse distribution. The initial and boundary conditions for both sets of experiments were obtained from actual historical atmospheric conditions during the event, provided by NCEP-FNL Operational Global Analysis data at $1^\circ \times 1^\circ$ resolution at every 6 h. In order to facilitate smooth interpolation of this coarse-resolution, global data, we used a three level nesting scheme shown in Fig. 5 (shown for the case of Mumbai City). Only the innermost (5 km) grid was subjected to further analysis. In this scenario instead of Noah-LSM, we used the 5 layer thermal diffusion scheme (originally developed for the MM5 model, therefore also known as MM5-scheme), in order to save computing time. This model is further explained in Skamarock et al. (2005).

4.1. Details of implementing landuse change by urbanisation

Conducting a non-idealised WRF/Noah simulation can be divided into three steps (NCAR et al., 2000): 1. Setting up of the model domain and static data. 2. Creating 3D initial and boundary condition data and 3. Running the model. In this set of experiments we conducted all three steps using standard data for the 'Present scenario'. The domain files of the step 1 of the 'Present scenario' were modified by changing only their vegetation fraction and albedo values to obtain the 'Future scenario'. We decreased albedo by 20% and vegetation fraction by 75% of the average background values to indicate the transition from non-urban to urban landuse. These values are in agreement with past experimental and theoretical studies (Royer et al., 1988). These changes were implemented in the modelling as follows: WRF model's pre-processor calculates the vegetation fraction and albedo (among other parameters) based on landuse data, when preparing the input files for the model. Instead of changing the input landuse maps, we directly modified these input file to change vegetation fraction and albedo. Then the resulting data was used to perform steps 2 and 3 for 'Future' scenario. Therefore the only difference of 'Future' scenario from the 'Present' is the decreased albedo and vegetation fraction.

4.2. Model validation

Each case was first run for the 'Present' scenario and the rainfall outcome was compared against reported events. However, this was only a qualitative comparison, to check whether the model produces a rainfall distribution that is

Table 2
Cities selected for the semi-idealised urbanisation sensitivity experiment.

City	Country/region	Population (millions)	Area sq. km	Event type	Period[1]
Colombo	Sri Lanka/South Asia	6	37	Monsoon, flood.	2–7/May/2007
Dhaka	Bangladesh/South Asia	13	304	Monsoon, flood.	7–17/Jul/2007
Mumbai	India/South Asia	14	438	Monsoon, flood.	1–6/Jul/2007
Taipei	Taiwan/South-east Asia	2.6	271	Monsoon, Flood.	6–10/Oct/2008

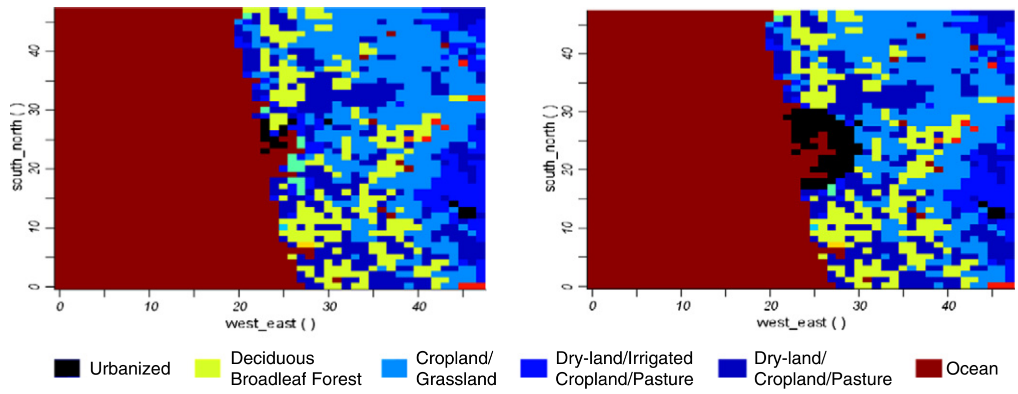

Fig. 4. The landuse transformation introduced in the semi-idealised study for the case of Colombo, Sri Lanka. Left: current, right: transformed.

similar to the event documented, as it was difficult to obtain suitable rainfall data for all the events for a better validation. As an example the accumulated rainfall over the 2007 May rainfall event in Colombo is shown in Fig. 6. This event recorded 12 cm rainfall at the only meteorological station in the city of Colombo. While the model could clearly reproduce the extreme rainfall condition around the city, the results are underestimated over the city centre. The highest rainfall values are further inland. However this discrepancy between point-measurements and spatial estimates is quite common due to a number of reasons like scaling issues (Pathirana and Herath, 2003, Shem and Shepherd, 2009). While there are many techniques to improve the forecasting outcome of this model, especially in an operational setting (e.g. assimilation of local sounding and surface data), they are not within the scope of this work.

4.3. Results

For each city we compared the rainfall output during the whole event for the cases of 'Present' and 'Future' scenarios.

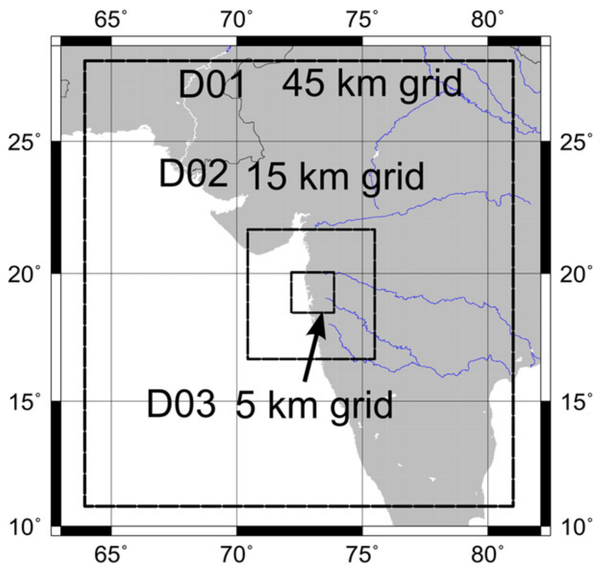

Fig. 5. Nesting scheme used for semi-idealised studies. The case of Mumbai City is shown.

Fig. 7 shows the quantile–quantile plots for each city. These plots were calculated by ordering non-zero grid level rainfall in ascending order and dividing into 100 equal quantiles. Cities of Colombo, Dhaka and Mumbai showed a significant increase of high-intensity rainfalls though the lower-intensities where largely unchanged. However, Taipei did not show any significant change of rainfall due to increased urbanisation.

All cases, including Taipei showed elevation of maximum recorded temperature (daytime) during the simulation period, but the minimum (night-time) temperature remained unchanged. The cases of Dhaka and Taipei are shown in Fig. 8.

5. Urban growth model

The urbanisation scenarios used in the previous semi-idealised case were crude — we simply assumed that the city will grow twice its current diameter and the area will be completely covered with urban landuse. In some cases this might be an approximation of the actual urban growth behaviour; since the 1980s, the city of Beijing, China, experienced a tremendous growth which follows an almost perfect radial expansion. Yet, urban growth patterns depend on numerous factors ranging from ground price distribution to physical conditions (e.g. slope and soil conditions). During the last forty years considerable progress has been made in accurately modelling spatially explicit urban development that mimics actual observations over space and time (White and Engelen, 1993; Makse et al., 1995; Ward, 2000; Filho et al., 2009 among many others) and a number of theories like diffusion limited growth (Makse et al., 1995) and cellular-automata (Ward, 2000) has been used as a basis for these models. While initially urban growth was treated like an almost generic phenomenon, currently urban growth models derive transition rules that mimic landuse or land cover changes from historical land use data of actual cities (e.g. Li and Yeh, 2000; Yang et al., 2008). After an initial training phase in which specific local growth patterns are 'learned', prospective growth is determined for future years. Apart from local growth dynamics, top-down information expressing planning constraints (e.g. zoning maps), physical conditions (e.g. variations in slope) and other factors (proximity to infrastructure, economic hotspots, etc.) are used to reflect actual conditions. Depending on the available

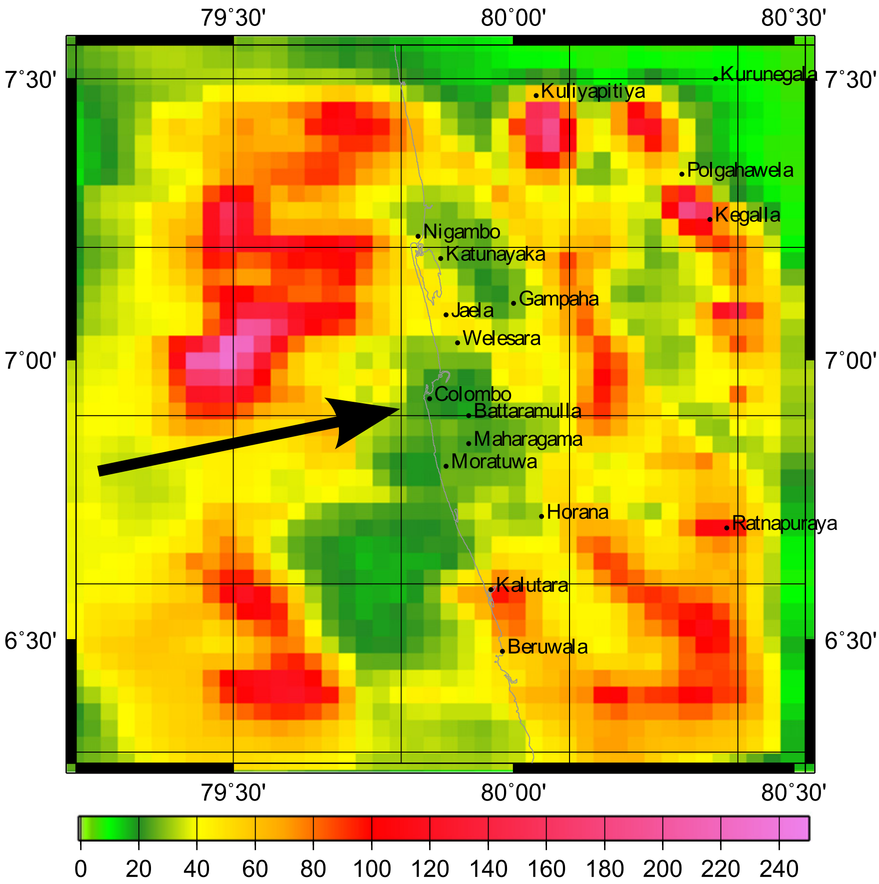

Fig. 6. Accumulated rainfall (mm) from 2 to 3 May 2007 rainfall event simulation. The prevailing surface wind direction is marked by the arrow.

data and planning consistency in cities, current urban growth models reach a relatively high level of accuracy; i.e. retrospective predictions are similar to observed land cover or landuse maps.

To explore the future urban growth extent for the city of Mumbai, we used the urban growth modelling platform Dinamica-EGO (Filho et al., 2009) to project the urban growth of the city of Mumbai based on its past urban growth characteristics. The process of building and validation of the urban growth models for Mumbai and several other cities are explained by Veerbeek et al. (2011). We used a maximum likelihood classification method to derive landuse classifications for city and surroundings of Mumbai for the base years 1992 and 2005 (Fig. 9). Using two significantly apart base years (1992 and 2005) the model derived transition rules to predict the urban extent for the year 2035 based on a 'business-as-usual (BAU)' assumption.[1] To derive the proper transition rules, additional base maps were used with information on infrastructure, morphology (slope, elevation), surface water and rivers, etc. Calibration of the model resulted in an 85% accuracy on a scale level of 240 × 240 m (Veerbeek et al., 2011). Higher levels of accuracy might be reached using a more intricate land cover classification process in combination with additional data on economic development, ground price differentiation and planning policies.

6. Mumbai case-study with future urbanisation

For the chosen areas, the urban extent of Mumbai and its suburbs increases in 2006 by about 22% (to 485 km^2) compared to the base year 1992 (398 km^2). The growth model estimates a less substantial one for the midterm year of 2035 (Veerbeek et al., 2011) in which the urban extent further increases by about 13% (547 km^2). Urbanisation mainly takes places in the eastern part of Navi Mumbai and the northern city of Thane. While currently disjoint, the outcomes predict the cities to merge with Mumbai which has little possibilities for expansion to the south/west because of its location on a peninsula.

WRF model routinely uses USGS landuse data, which covers the globe at a resolution of about 1 km. Our landuse model based data is of a much higher resolution, but has its own sources of uncertainties and errors (e.g. classification errors). Using USGS data for the 'Present' situation and landuse model predictions for 'Future' case does not provide a fair basis for investigating the impact of future urbanisation due to the very different nature of the two data sources. Therefore, we investigated the influence of landuse

[1] BAU assumption: The transition rules derived from the past apply to the future.

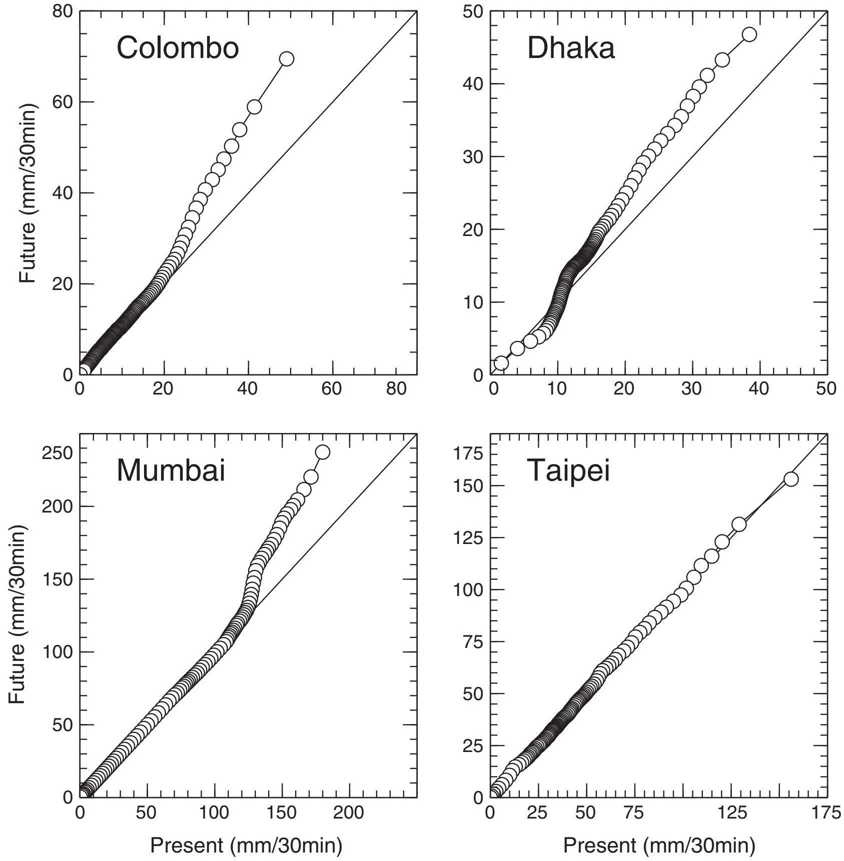

Fig. 7. Quantile–Quantile plots rainfall from model output. The non-zero grid-level rainfall values were sorted and divided into 100 equal quantiles.

on extreme rainfall events by using 1992 and 2035 landuse patterns as follows.

As explained in Section 4, the outermost domain of a mesoscale model has to be fairly large, in-spite of the fact that the area of interest (covered by innermost grid) is only a few thousand square kilometres. For this numerical experiment we constructed three nested domains with resolutions 30 km, 6 km and 1.2 km, covering areas of 100 × 100, 121 × 121 and 46 × 56 grids. The urban growth model covers only a space of approx. 1700 km^2, which is about half of the area of the innermost domain. We used the 24 category USGS landuse data to first create the simulation domain. Then for both 'Present' and 'Future' scenarios, this landuse data was patched with the respective model-based landuse patterns (Fig. 9), and translated into USGS conventions. The procedure of patching is illustrated in Fig. 10. Then for each grid-cell that was originally non-urban in USGS data, but urban in the patched data, we decreased the albedo by 20% and vegetation fraction by 75%. For partially urbanised cells we reduced the quantities by a percentage C given by,

$$C = \frac{U_{\mathrm{mode1}}}{U_{\mathrm{USGS}}} C_0 \qquad (1)$$

where U_{model} and U_{USGS} are the urban landuse fraction of the cell according to patched landuse and original USGS landuse data, respectively. C_0 is 25% for albedo and 75% for vegetation fraction.

In this simulation we used WRF model with the Noah land surface model to represent the surface processes. No cumulus parameterisation was used for the innermost domain as the grid size of the domain is small enough to fully explicitly resolve the cumulus formation, by means of cloud microphysics. Important model parameters are given in Table 4.

The model was integrated for four historical rainstorms that caused flooding (Table 3), under 'Present scenario' and 'Future scenario' conditions. Fig. 11 shows the quantile–quantile plots for the rainfall simulations for these cases. Quantiles were calculated by sorting grid level rainfall in descending order and dividing into 100 equal quantiles.

Based on the simulation experiments for the four events, we attempted to analyse the possible change in the extreme precipitation frequencies. We based our analysis on the intensity–duration–frequency formula for Western India proposed by Kothyari (1992):

$$I_t^T = 8.3 \frac{T^{0.2}}{t^{0.71}} \left(R_{24}^2\right) \qquad (2)$$

where I_t^T is the intensity of rainfall in mm/h, T is the return period in years and t is the duration in hours. R_{24}^2 is the magnitude of the two year return period, 24 h duration

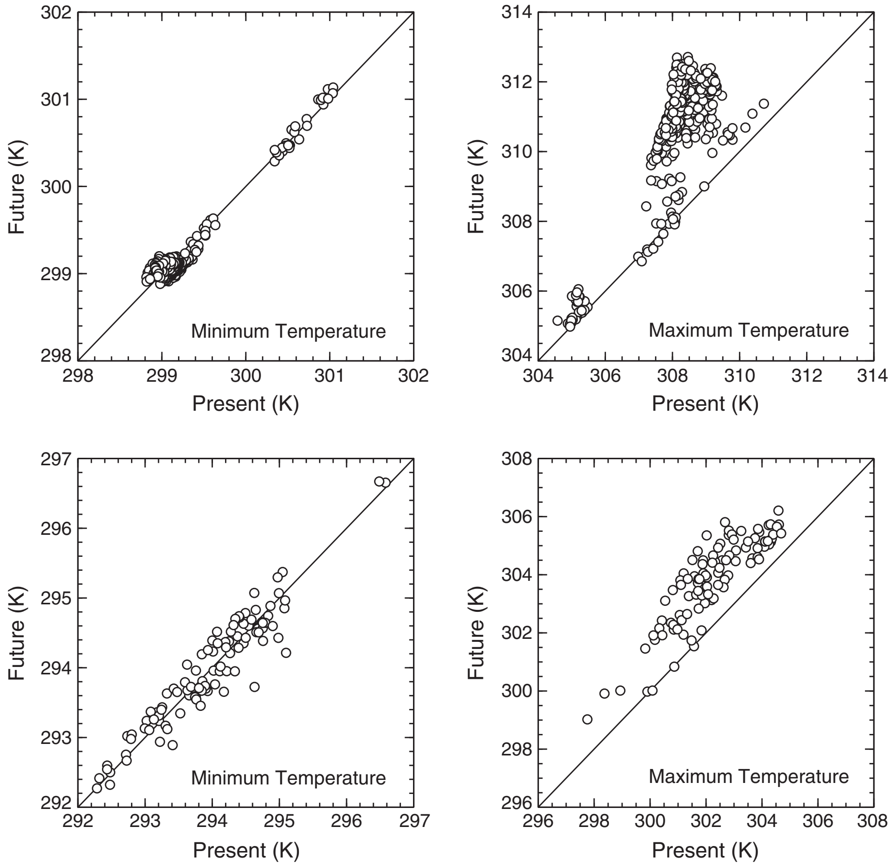

Fig. 8. Simulated maximum (daytime) and minimum (night-time) temperature in Dhaka (top) and Taipei (bottom) during the event.

rainfall event volume in mm. Kelkar (2005) estimates the two year return period rainfall in Mumbai as 200 mm. Instead of 15 min time interval used for reporting the results of the rest of the study, we used 1 h as the storm-duration for the frequency analysis so that it is possible to compare the results of our analysis with commonly measured rainfall. We performed a quantile–quantile analysis of all events (500 equal quantiles). Then each of the 'Future' and 'Present' quantiles was given a return period based on Eq. (2). Fig. 12 shows the resulting relationship of the return periods. According to our findings, the current 10-year rainfall event (75 mm/h) would increase its frequency to a 3 year recurrence and 50-year (105 mm/h) to 22-year.

7. Synthesis

We performed three sets of numerical experiments in order to test the hypothesis that changes in urban landuse cause significant changes in extreme rainfall in urban centres and surrounding areas. The first experiment was a completely idealised one set up within a quasi-2D domain with periodic boundary conditions. Keeping all other parameters constant, we changed the size of the urban landuse patch on the domain. The high rainfall yield over a 60 km area starting from the centreline of the city showed a significant positive trend with increasing urban landuse. However, the windward stretch of the city showed a significant reduction of high rainfall. This latter phenomenon can easily be explained by the use of periodic boundary condition and the limited extent of the modelling domain. Due to limited replenishment of moisture (small 'ocean' area), heavy rainfall in one part of the domain would naturally result in the reduction of rainfall in another part.

In real-world cities, the meteorological situation involves a number of complexities like impact of topography and water bodies, changes in wind direction with time, location and elevation and the surface properties are also much more heterogeneous. Therefore it is conceivable that the rainfall response to urbanisation also should be quite complicated in real cities, compared to this idealised study. However, it is remarkable that even under these ideal conditions, the response of the system to the increased urbanisation was far from straight-forward monotonically increasing one. There are instances where increasing urbanisation, indeed, caused a reduction in high rainfall yield (e.g. urban patch size increase from 8 km to 12 km (Fig. 2)). Considering the design of the experiment (we repeated each simulation ten times with slightly different initial conditions) it is hard to attribute this to the complex-system response–sensitive dependence on the initial condition of the system. Seemingly this is a real feature of the response of rainfall process to UHI growth. Kusaka et al. (2009) discussed a chaotic response of the

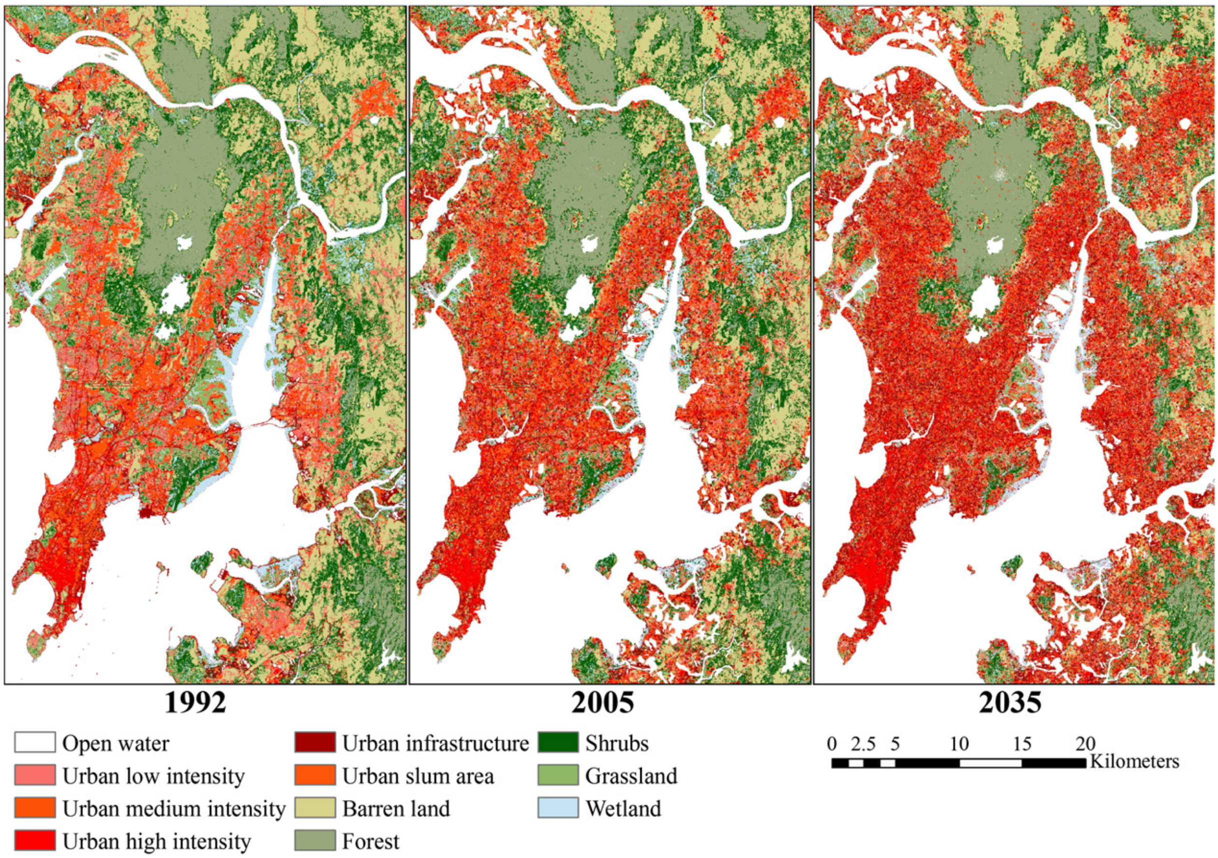

Fig. 9. Landuse classifications derived from LandSAT data (1992, 2005) and Dynamica EGO simulation (2035).

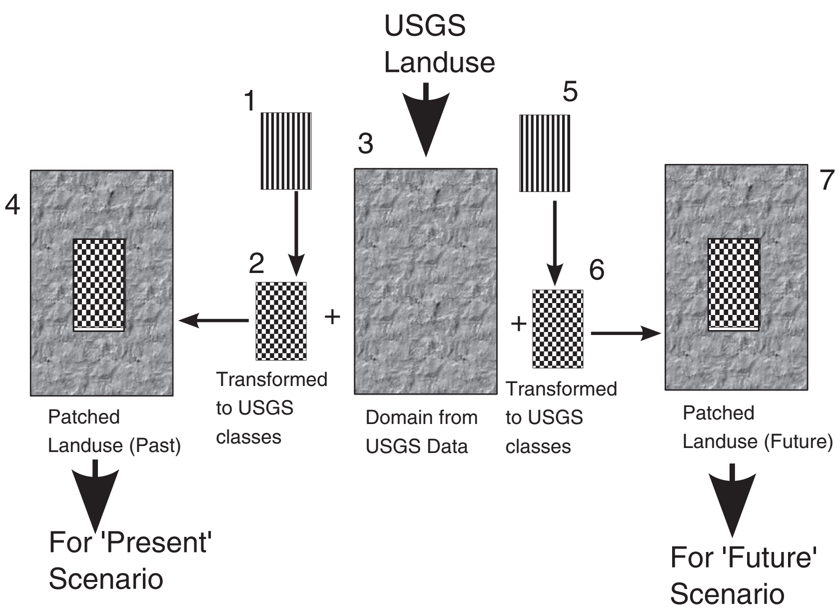

Fig. 10. The landuse patching process. (1) 'Present scenario' landuse map produced by urban growth simulation model, based on its own landuse classes. (2) Same map transformed to USGS 24 category classes. (3) The landuse map created using original USGS landuse data. (4) The patched landuse map used in WRF model simulations for 'Present scenario'. (5),(6),(3) and (7): same procedure for 'Future scenario'.

Table 3
Mumbai rainfall events simulated.

Event	Event date	Simulation	
		Start	End
Event 1[a]	–	2010-08-22 00:00	2010-08-24 18:00
Event 2	2010-08-30	2010-08-27 00:00	2010-08-30 00:00
Event 3	2007-07-03	2007-07-01 00:00	2007-07-06 18:00
Event 4	2005-07-26	2005-07-24 00:00	2010-08-24 18:00

[a] A large scale event that caused rainfall in many locations in India.

atmospheric field to landuse change. The non-linear dependence of rainfall activity to the urban size may have resulted from a similar response of the model atmosphere.

One of the signature features of urbanisation is the reduction of the latent heat released by the surface to the upper atmosphere (Fig. 13). The urban landuse typically causes low latent heat release due to the low transpiration as well as low rainfall interception (Nakayoshi et al., 2009) compared to vegetated surfaces. This is one of the major causes of excessive thermal built-up near the surface triggering convective breakup during the daytimes. In these instances the air circulation above the city acts as a virtual mountain, lifting the large-scale wind fields. All simulations in the three sets of experiments showed this behaviour (e.g. Fig. 8). However, the situation is not as straightforward when the UHI causes the rainfall to be enhanced over the city (e.g. Charabi and Bakhit, 2011). The rain increases moisture availability, and could in turn increase the latent heat release by urban landuse. To what extent this would offset the reduction of transpiration depends on a number of factors: The amount of solar radiation (affecting potential evaporation) and the moisture availability (depending on rainfall and surface runoff) are two major ones.

There are many more realistic versions of the radiative transfer. The WRF model has an urban canopy parameterisation scheme that allows for canyon effects of buildings on radiation and winds to be implemented (Salamanca and Martilli, 2010). COAMPS model already uses this in operational simulations (Meir et al., 2013). In the present studies we did not employ that parameterisation scheme. The impacts of the landuse change is represented in the models only by its influence on the surface scheme — Noah-LSM in first and third cases or thermal diffusion in the second case. While Noah LSM has a simple parameterisation for this impact, these are not specifically detailed for urban environments (Lee et al., 2011). Further studies on explicit parameterisation methods to represent urban land-form accurately are much needed.

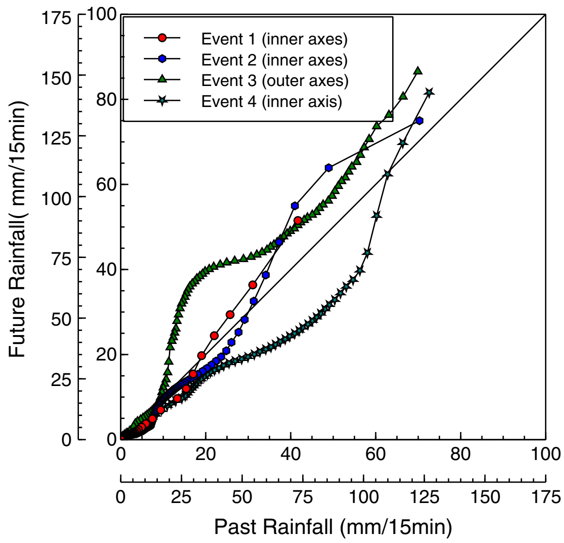

Fig. 11. Quantile–quantile plots of the simulations of four events in Mumbai.

Rainfall frequency analysis based on near-stationary data is a well established technique. Using those techniques for the purpose of demonstrating the changes of extreme values that may result as a change of the climatic system-be it global or regional — is a challenging, if not a seemingly impossible task. The effort towards the result shown in Fig. 12 involves some major assumptions. Extreme value analysis typically needs a long record of (annual) maximum rainfall at a given location, equivalent of which, is hard to obtain in the case of the 'what-if' experiments we have conducted. Instead, we sampled a number of model grid points in the general area of the Mumbai City to obtain a varied record of high-intensity rainfall values. The basis for this approach is explained by Pathirana (2011). While this may provide the necessary variability in a statistical sense, the fact remains that all of these values resulted from a few (in our case four) storm events. In a given climate extreme rainfall can be caused by a variety of meteorological situations (e.g. local-convective activity, monsoon, and cyclones) — all of which are impossible to be represented by a limited number of event simulations. For the case of Mumbai this situation is somewhat remedied by the fact that most of the extreme rainfall is caused by summer monsoon events like the ones we simulated. However, for other climates the situation may be much more complex demanding much larger number of simulations.

Table 4
Important WRF model parameters used in three sets of experiments.

Parameter	Idealised study	Semi-idealised study	Mumbai case
Microphysics	MM5 — Lin et al.		
Short-wave radiation	MM5 — Dudhia scheme		
Long-wave radiation	RRTM scheme		
Surface-layer physics	Noah-LSM with 4 soil layers	MM5 — 5 layer thermal diffusion model	Noah-LSM with 4 soil layers
Boundary layer physics	YSU scheme		
Cumulus parameterisation	None	Betts–Miller–Janjic (outer domains) No cumulus scheme (inner domain)	

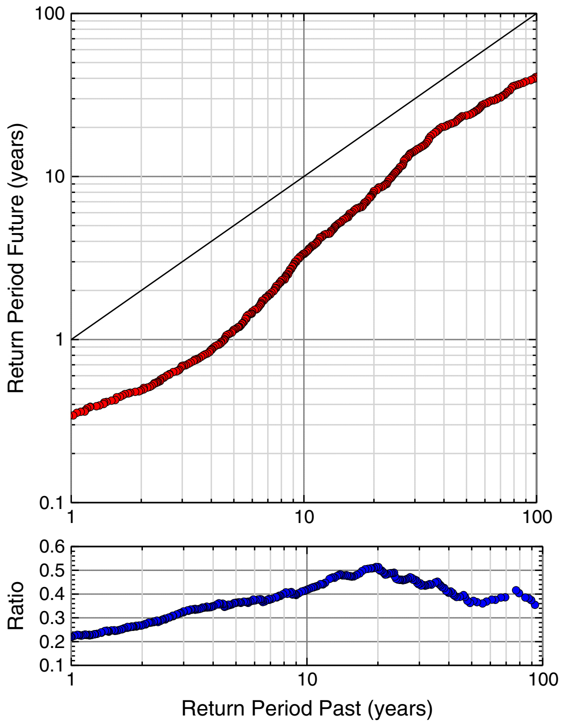

Fig. 12. Top: frequencies of extreme rainfall for current and future scenarios. Bottom: the ratio of (Future Return Period)/(Past Return Period). The frequency of current 10 year magnitude storm would be 3 years and 100 year would be 30 years.

The results of urbanisation are markedly different for different cities. Cities may grow in quite unplanned fashion where much of the vegetation is removed only to be replaced by urban sprawl. On the other hand planned urbanisation might allow for green spaces that would — among other benefits — improve the release of latent heat reduce the heat island build-up. The way we have parameterised and modelled the urban change is simple compared to the actual reality. Probably the level of enhancement of rainfall due to urban heat island in reality could be somewhat overestimated by these experiments. However, we believe that the evidence produced is adequate to prove the hypothesis that extensive urbanisation can cause changes in rainfall in and around cities. Further, we have shown that these changes concentrate around extreme rainfall quantities, compared to small rains. The implications of this should be considered in urban planning activities, particularly in designing new urban drainage infrastructure that is expected to last for at least several decades. The more accurate quantification of the changes requires further research.

There are many indications, that the relationship of urban heat island caused rainfall enhancement, to the increase of urbanisation, while being a significant and positive one, is far from simple. For example our idealised experiments showed some instances where a certain level of increase in urbanisation resulted in a net decrease of rainfall (Fig. 2). Our simulation with Taipei did not show any sensitivity of rainfall to doubling the city's diameter. A plausible explanation for this might be the fact that the complex surrounding topography involving mountains already play a significant role in precipitation formation (Lin et al., 2008), and further increase of the urban patch does not contribute to a further enhancement of precipitation.

In the case of Mumbai the July 2007 storm magnitude (Fig. 14) increased over the urban area, but the large precipitation on the north of the city was slightly reduced in the ‘Future’ scenario. In a different study Ntelekos et al. (2008) have concluded that the severe 2004 July rainstorm over Baltimore did not show a sensitivity to UHI. The dynamics of the urban heat island formation and the resulting changes in the rainfall are complex and depend on a multitude of localised parameters like topography, surrounding landuse, and features of the local/seasonal climatic regime. In order to make more reliable predictions on the impact each locality should be studied in detail. It is difficult to generalise the results at the

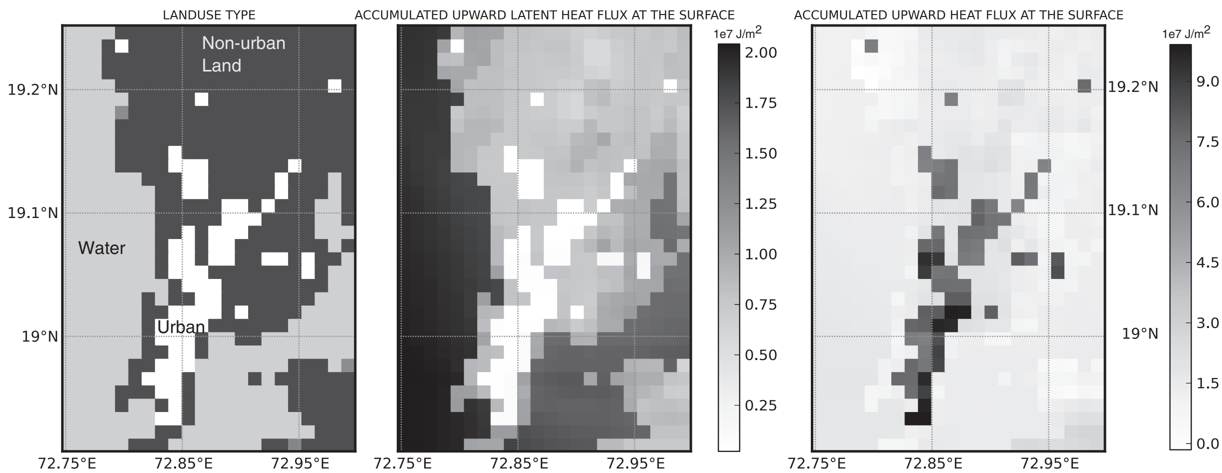

Fig. 13. Accumulated latent heat flux (centre) and accumulated sensible heat flux (right) for 2005 July Mumbai case (Event 4), ‘Present scenario’. Corresponding landuse map (simplified) is shown on the left. Urban areas decrease the latent heat flux dramatically, while increasing sensible heat flux.

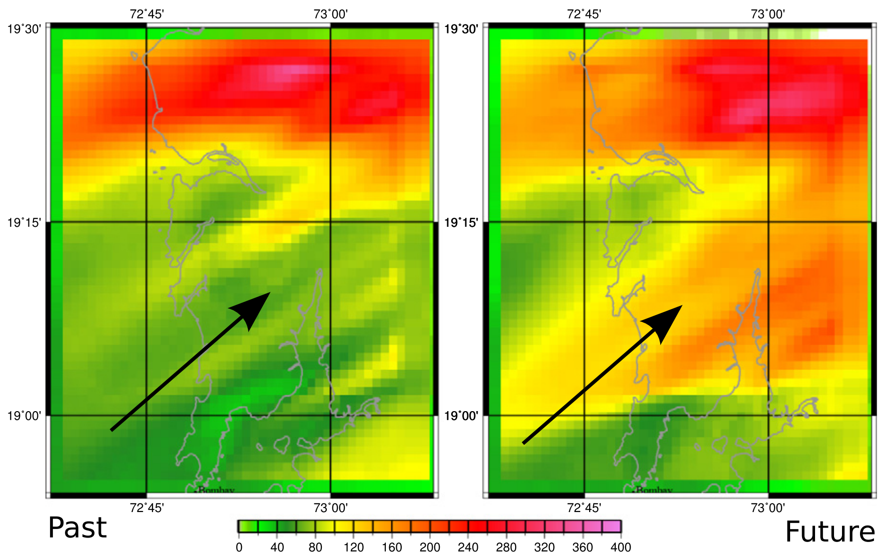

Fig. 14. Total rainfall accumulations (mm) during the 2007 July rainfall event simulation. The prevailing surface wind direction is marked by the arrow.

global or even at the regional level. This is an area that deserves further attention of the climate research community.

Appendix A. Supplementary data

Supplementary data to this article can be found online at http://dx.doi.org/10.1016/j.atmosres.2013.10.005.

References

Changnon Jr., S.A., 1979. Rainfall changes in summer caused by St. Louis. Science 205, 402–404.

Charabi, Yassine, Bakhit, Abdelhamid, 2011. Assessment of the canopy urban heat island of a coastal arid tropical city: the case of Muscat, Oman. Atmos. Res. 101 (1), 215–227.

Doyle, J.D., Durran, D.R., 2001. The dynamics of mountain wave induced rotors. J. Atmos. Sci. 59, 186–201.

Filho, B.S.S., Rodrigues, H.O., Costa, W.L.S., 2009. Modeling Environmental Dynamics with Dinamica EGO. Instituto de Geociencias-Centro de Sensoriamento Remoto, Av. Antonio Carlos, Universidade Federal de Minas Gerais-Campus Pampulha.

Foley, J.A., DeFries, R., Asner, G.P., Barford, C., Bonan, G., Carpenter, S.R., Chapin, F.S., Coe, M.T., Daily, G.C., Gibbs, H.K., Helkowski, J.H., Holloway, T., Howard, E.A., Kucharik, C.J., Monfreda, C., Patz, J.A., Prentice, I.C., Ramankutty, N., Snyder, P.K., 2005. Global consequences of land use. Science 309 (5734), 570–574.

Jauregui, E., 1996. Urban effects on convective precipitation in Mexico city. Atmos. Environ. 30 (20), 3383–3389.

Kawabata, T., Seko, H., Saito, K., Kuroda, T., Tamiya, K., Tsuyuki, T., Honda, Y., Wakazuki, Y., 2007. An assimilation and forecasting experiment of the Nerima heavy rainfall with a cloud-resolving nonhydrostatic 4-dimensional variational data assimilation system. J. Meteorol. Soc. Jpn. 85 (3), 255–276.

Kelkar, R.R., 2005. Understanding the extreme weather events. Newslett. Indian Water Resour. Soc. (November).

Kishtawal, C.M., Niyogi, D., Tewari, M., Pielke, R.A., Shepherd, J.M., 2010. Urbanization signature in the observed heavy rainfall climatology over India. Int. J. Climatol. 30 (13), 1908–1916.

Kothyari, U., 1992. Rainfall intensity duration frequency formula for India. J. Hydraul. Eng. ASCE 118 (2), 323–336.

Kusaka, H., Kimura, F., Nawata, K., Hanyu, T., Miya, Y., 2009. The chink in the armor: questioning the reliability of conventional sensitivity experiments in determining urban effects on precipitation patterns. The 7th International Conference on Urban Climate, vol. 29 (June).

Landsberg, H.E., 1981. The urban climate. International Geophysics, vol. 28. Academic Press.

Lee, S.H., Kim, S.W., Angevine, W.M., Bianco, L., McKeen, S.A., Senff, C.J., Trainer, M., Tucker, S.C., Zamora, R.J., 2011. Evaluation of urban surface parameterizations in the WRF model using measurements during the Texas air quality study 2006 field campaign. Atmos. Chem. Phys. 11 (5), 2127–2143.

Li, L., 2006. Atmospheric GCM response to an idealized anomaly of the Mediterranean sea surface temperature. Clim. Dyn. 27, 543–552. http://dx.doi.org/10.1007/s00382-006-0152-6.

Li, Xia, Yeh, Anthony Gar-On, 2000. Modelling sustainable urban development by the integration of constrained cellular automata and GIS. International Journal of Geographical Information Science 14 (2), 131–152.

Lin, C.Y., Chen, W.C., Liu, S.C., Liou, Y.A., Liu, G., Lin, T., 2008. Numerical study of the impact of urbanization on the precipitation over Taiwan. Atmos. Environ. 42 (13), 2934–2947.

Lin, W., Zhang, L., Du, D., Yang, L., Lin, H., Zhang, Y., Li, J., 2009. Quantification of land use/land cover changes in Pearl River Delta and its impact on regional climate in summer using numerical modeling. Reg. Environ. Change 9 (2), 75–82.

Lowry, W.P., 1998. Urban effects on precipitation amount. Prog. Phys. Geogr. 22 (4), 477–520.

Makse, H.A., Havlin, H., Stanley, H.E., 1995. Modelling urban growth. Nature 277, 608–612.

Meir, Talmor, Orton, Philip M., Pullen, Julie, Holt, Teddy, Thompson, William T., Arend, Mark F., 2013. Forecasting the New York City urban heat island and sea breeze during extreme heat events. Weather Forecast. http://dx.doi.org/10.1175/WAF-D-13-00012.1 (e-View).

Mitchell, K., 2000. The community Noah land-surface model (LSM): users guide. Technical Report. National Centers for Environmental Prediction (NCEP), USA.

Nakayoshi, M., Moriwaki, R., Kawai, T., Kanda, M., 2009. Experimental study on rainfall interception over an outdoor urban-scale model. Water Resour. Res. 45, W04415. http://dx.doi.org/10.1029/2008WR007069.

NCAR, NCEP, FSL, AFWA, the Naval Research Laboratory, NOAA and FAA, Weather Research and Forecasting Model Website, 2000. (Last accessed: Oct 2013).

Ntelekos, Alexandros A., Smith, James A., Lynn Baeck, Mary, Krajewski, Witold F., Miller, Andrew J., Goska, Radoslaw, 2008. Extreme hydrometeorological events and the urban environment: dissecting the 7 July 2004 thunderstorm over the Baltimore MD Metropolitan Region. Water Resour. Res. 44 (8).

Pathirana, A., 2011. Pitfalls in using the historical record (or 'stationarity is dead'). In: Zevenbergen, C., Cashman, A., Evelpidou, N., Pasche, E., Garvin, S., Ashley, R. (Eds.), Urban Flood Management. CRC Press/ Balkema Taylor & Francis Group, London, pp. 54–59.

Pathirana, A., Herath, S., 2003. Multifractal modelling and simulation of rain fields exhibiting spatial heterogeneity. Hydrol. Earth Syst. Sci. 6 (4), 695–708.

Pathirana, A., Herath, S., Yamada, T., 2005. Simulating orographic rainfall with a limited-area, non-hydrostatic atmospheric model under idealized

forcing. Atmospheric Chemistry and Physics, 5. European Geosciences Union 215–226.
Pathirana, A., Herath, S., Yamada, T., Swain, D., 2007. Impacts of anthropogenic aerosols on south Asian rainfall — a modeling study. Clim. Change 85 (1–2), 103–118.
Royer, Alain, Charbonneau, Lise, Teillet, Philippe M., 1988. Interannual Landsat-MSS reflectance variation in an urbanized temperate zone. Remote Sens. Environ. 24 (3), 423–446.
Sagan, C., 2000, O.B., Pollack, J.B., 1979. Anthropogenic Albedo changes and the Earth's climate. Science 206 (4425), 1363–1368.
Salamanca, F., Martilli, A., 2010. A new building energy model coupled with an urban canopy parameterization for urban climate simulations part II. Validation with one dimension off-line simulations. Theor. Appl. Climatol. 99 (3), 345–356.
Shem, W., Shepherd, M., 2009. On the impact of urbanization on summertime thunderstorms in Atlanta: two numerical model case studies. Atmos. Res. 92 (2), 172–189.
Shepherd, J.M., 2005. A review of current investigations of urban-induced rainfall and recommendations for the future. Earth Interact. 9 (12), 1–27.
Shepherd, J.M., 2006. Evidence of urban-induced precipitation variability in arid climate regimes. J. Arid Environ. 67 (4), 607–628.
Skamarock, W.C., Klemp, J.B., Dudhia, J., Gill, D.O., Barker, D.M., Wang, W., Powers, J.G., 2005. A description of the advanced research WRF version 2. Technical Report. National Center for Atmospheric Research, Bounlder, Colorado, USA.
Solomon, S., Qin, D., Manning, M., Chen, Z., Marquis, M., Averyt, K.B., Tignor, M., Miller, H.L. (Eds.), 2005. Climate Change 2005 — The Physical Science Basis: Working Group I Contribution to the Fourth Assessment Report of the IPCC. Cambridge University Press, Cambridge, UK and New York, NY, USA.
Subbiah, S., Vishwanath, V., Kaveri Devi, S., 1990. Urban climate in Tamil Nadu, India: a statistical analysis of increasing urbanization and changing trends of temperature and rainfall. Energy Build. 15 (1–2), 231–243.
Taha, H., Akbari, H., Rosenfeld, A., Huang, J., 1988. Residential cooling loads and the urban heat island — the effects of albedo. Build. Environ. 23 (4), 271–283.
Takahashi, H., 2003. Secular variation in the occurrence property of summertime daily rainfall amount in and around the Tokyo Metropolitan area. Tenki 49, 31–41 (In Japanese, with abstract in English).
Veerbeek, W., Denekew, H.B., Pathirana, A., Bacchin, T., Brdjanovic, D., 2011. Urban growth modeling to predict the changes in the urban microclimate and urban water cycle. 12th International Conference on Urban Drainage Modelling. Brazil.
Ward, D., 2000. A stochastically constrained cellular model of urban growth. Comput. Environ. Urban Syst. 24 (6), 539–558.
Watkins, Richard, Kolokotroni, Maria, 2013. The London Urban Heat Island — Upwind Vegetation Effects on Local Temperatures. PLEA2012 — 28th Conference, Opportunities, Limits & Needs Towards An Environmentally Responsible Architecture; Lima, Perú 7–9 November 2012.
White, R., Engelen, G., 1993. Cellular automata and fractal urban form: a cellular modelling approach to the evolution of urban land-use patterns. Environ. Plan. A 25 (8), 1175–1199.
Yang, Qingsheng, Xia, Li, Xun, Shi, 2008. Cellular automata for simulating land use changes based on support vector machines. Computers & geosciences 34 (6), 592–602.